



Chemically modified babassu coconut (*Orbignya sp.*) biopolymer: characterization and development of a thin film for its application in electrochemical sensors

Paulo Ronaldo Sousa Teixeira^{1,2} · Ana Siqueira do Nascimento Marreiro Teixeira^{1,2} · Emanuel Airton de Oliveira Farias³ · Durcilene Alves da Silva^{1,3} · Lívio César Cunha Nunes⁴ · Cleide Maria da Silva Leite⁵ · Edson Cavalcanti da Silva Filho¹ · Carla Eiras^{1,3} 

Received: 8 November 2017 / Accepted: 16 April 2018
© Springer Science+Business Media B.V., part of Springer Nature 2018

Abstract

The babassu coconut is a plant very abundant in northeast of Brazil and other countries, and any part of plant and fruit becomes residue. In this study, babassu mesocarp (*Orbignya sp.*) (BM) was chemically modified with phthalic anhydride (BMPA) to increase its solubility in an aqueous medium, and thus facilitate its processing in the form of thin films. The reaction of modification of the babassu mesocarp with phthalic anhydride (PA), obtaining BMPA, was confirmed by FTIR, XRD, TG/DTG, Zeta Potential and SEM analysis, from the differences in the bands of the FTIR spectra, increase in crystallinity, new thermal profile, changes in zeta potential value and morphology, respectively. The thin monolayer films of BM and BMPA were produced by the self-assembly monolayer (SAM) technique, and adsorbed onto conductive glass substrates (tin-doped indium oxide, ITO). The electroactive properties of these thin films were evaluated by cyclic voltammetry (CV). BM exhibited a pair redox pair process of +0.57 V (oxidation) and +0.19 V (reduction) for BM. In BMPA these redox processes were observed at +0.37 V (oxidation) and 0.24 V vs. ECS (reduction), verifying that both BM and BMPA are electroactive materials that can be used in the construction of sensor platforms, without the necessity of being conjugated with other electroactive materials, such as conductive polymers, metal phthalocyanines, or dyes. Furthermore, under the experimental conditions used, the BMPA presented a more reversible redox process and higher electrochemical stability in

Highlights

- Babassu mesocarp (BM) was chemically modified with phthalic anhydride (BMPA)
- BM and BMPA were characterized by FTIR, XRD, TGA, zeta potential, and SEM
- Thin films based on BM or BMPA were produced by Layer-by-Layer technique
- The chemical modification improved BM reversibility and electrochemical stability.
- BM and BMPA presented electroactivity and can be used in sensor platforms.

✉ Carla Eiras
carla.eiras.ufpi@gmail.com

¹ UFPI, Interdisciplinary Laboratory for Advanced Materials (LIMAV), Teresina, Piauí 64049-550, Brazil

² IFPI, Federal Institute of Education, Science and Technology of Piauí, Teresina, Piauí, 64000-040, Brazil

³ UFPI, Research Center in Biodiversity and Biotechnology – Biotech, University of Piauí, Parnaíba, Piauí, Brazil

⁴ UFPI, Center for Pharmaceutical Technology, Federal University of Piauí, Teresina, Brazil

⁵ UNILAB University of International Integration of Afro-Brazilian Lusophony, Acarape, Ceará Icen, 62785-000, Brazil

comparison to BM. This effect occurs because BMPA has higher solubility in aqueous media, which favors the preparation of films with smaller grain sizes compared to BM films, as observed by Atomic Force Microscopy (AFM). This study showed that BMPA is a new material with potential for applications in electrochemical sensors.

Keywords Babassu mesocarp · Phthalic anhydride · Thin films · Electroactivity

Introduction

Natural polymers, are defined as polymers obtained within the cells of living organisms by complex metabolic processes [1]. They can be structurally classified as polysaccharides, polyesters, and polyamides. These materials degrade by themselves as a result of the actions of living organisms and/or enzymes, and generate carbon dioxide, water, and biomass [2].

Recently, natural polymers have received special attention from the scientific community, as well as the petroleum, drug, and food industries [1], due to their important specific properties such as biodegradability and biocompatibility [3], which are properties not available in most currently known synthetic polymers [4, 5]. Natural polymers, such as chitosan [5, 6] can be used as a matrix for their application in controlled-release devices, and in environmentally sensitive membranes, as is the case for cellulose [7].

The main raw materials needed to obtain natural polymers include renewable carbon sources, which are generally derived from commercial large-scale plantations of sugarcane, corn, potatoes, wheat, sugar beet, and sunflower, among others [8]. Other sources of natural polymers are lignocellulosic materials, which are formed by rigid and fibrous structures composed mainly of cellulose, hemicellulose intermingled with lignin through covalent and hydrogen bonds [9].

The babassu palm tree (*Orbignya* sp) (Fig. 1a) is abundant in Brazil, region known as “mata dos cocais”, in the states of Maranhão, Tocantins, and Piauí [10]. It has a large and cylindrical trunk, with a crown with fruits and coconuts of an ellipsoidal shape. This fruit contains epicarp, mesocarp,

endocarp, and almond at mass percentages of 11%, 23%, 59%, and 7%, respectively, as pictured in Fig. 1b [11].

Babassu mesocarp is characterized as a non-toxic and renewable material, and has a great potential to be used in industrial areas as a food supplement, and an excipient of drugs [12]. Similar to other lignocellulosic materials, BM is very reactive due to the available hydroxyl groups on the surface of the polysaccharides [13]. Due to this reactivity, the Babassu mesocarp can be modified with the insertion of several chemical groups on its structure, in order to incorporate on polymer matrix new characteristics.

The great advantage of insertion functional groups on the BM structure is the increased cation adsorption capacity [14]. In the BM modification process, the hydroxyls present in the starch, cellulose and hemicellulose can be converted into carboxyl groups using reagents such as succinic, phthalic, or maleic anhydrides [14].

A new applicability for BM comes from processing it in the form of thin films, fixed on solid substrates and conductors, in such a manner as to compose the active layer of an electrochemical sensor. The term “film” refers to condensed matter arranged in immobilized layers onto a substrate [15]. Depending on their thickness, “thin films” can be classified as nanometric (0.1–100 nm), micrometric (0.1–100 μm), or millimetric (0.1–100 mm) [16].

Nanostructured films exhibit molecular organization and have nanometer scale dimensions (10^{-9} m). The organizational level of the molecules in the films depends on several parameters; among them, we considered the nature of the material under study and the processing technique used, and their respective experimental parameters [17].

Fig. 1 (a) Overview of the babassu palm tree, “mata dos cocais” (*Orbignya* sp). (b) Section of the babassu coconut: a - epicarp, b - mesocarp, c - endocarp, and d - almond



Among the different techniques for preparing thin films, the self-assembled monolayer (SAM) technique is characterized by a monolayer being adsorbed onto a substrate. This technique can be easily prepared by immersing the substrate in a diluted solution containing the molecule, or material of interest, for a specific amount of time. Additional steps of washing and drying (normally using N_2) can be effectuated [18].

The interest in films produced by the SAM technique in the construction of sensors is due to the high organization exhibited by the monolayers, which assures a homogeneous behavior throughout the electrode surface, contributing to the synthesis of sensors with a greater sensitivity and reproducibility. Furthermore, the monolayer dimension, which is located on a molecular scale, avoids the slow diffusion of the electroactive species to the surface, especially when compared to the kinetics presented by electrodes modified with thin polymer films or composites. [19].

According to what was presented, and taking into account the great availability of *Orbignya sp.* in Brazil and other countries, the present study aimed to synthesize BM and BMPA thin films using SAM for their future application in electrochemical sensors or biosensors.

Materials and methods

Materials

Babassu mesocarp was obtained as a powder from the Department of Agricultural Sciences at the Federal University of Piauí (Brazil), and then granulometry was performed to measure the grain size, which was approximately 0.074 mm. Analytical standard phthalic anhydride (PA) (Aldrich) and dimethylacetamide (DMAc) were obtained from Aldrich and used without further purification. The solution used during the film adsorption was produced by dissolving the BM powder in dimethyl sulfoxide (DMSO; Aldrich) and sulfuric acid (Aldrich), both of which were analytical standard, and used without their further purification.

Modification of the Babassu Coconut Mesocarp with Phthalic Anhydride

The modification of BM with phthalic anhydride (BMPA) was performed in the solid state using the lignocellulosic free carboxyl groups [20]. The reaction occurred in an oil bath at about 131 °C, which is the melting temperature of phthalic anhydride (PA), where BM and PA were mixed in a ratio of 1:5 (w/w), respectively. After the fusion of the reagents, the mixture was kept in agitation for 20 min, and the reaction was terminated by adding dimethylacetamide (DMAc) into the

reaction medium, and allowing the reaction vessel to cool to room temperature (24 °C) [21]. Afterwards, the product (BMPA) was separated by centrifugation, and sequentially washed with acetone and ultrapure water (milli-Q) to remove the excess phthalic anhydride. The final product was dried in a stove at 60 °C for 12 h. Fig. 2 shows the scheme for production of BMPA [21].

Determination of acidic groups of BMPA

The acid groups of BMPA was determined from the amount of carboxyl groups attached to the BM surface by employing the back-titration technique. For this, 0.1 g of BMPA were treated with 100 mL of aqueous NaOH (400 mg/dm³) in a 250 mL Erlenmeyer flask for 1 h under constant magnetic agitation. Then, the material was separated by simple agitation, and three rates (20 mL) from the obtained solution were titrated with an HCl solution (365 mg/dm³). The concentration of the carboxyl groups was calculated using Eq. 1 [21, 22],

$$C = \frac{(C_{NaOH} \times V_{NaOH}) - (5 \times C_{HCl} \times V_{HCl})}{M_{bio}} \quad (1)$$

where C_{NaOH} is the concentration of the NaOH solution (400,0 mg/dm³); C_{HCl} is the concentration of the HCl solution (365,0 mg/dm³); V_{NaOH} is the volume of NaOH (dm³) used; V_{HCl} is the volume of HCl spent on titration of excess base that did not (dm³); and M_{bio} is the mass of BMPA (g).

X-Ray diffraction– XRD

The X-ray Diffratograms was performed using a Shimadzu D600-XR, with 2θ in the 5–75° interval, at a scan speed of $8.33 \times 10^{-2} \text{ s}^{-1}$, and using a $CuK\alpha$ radiation source with a wavelength of 1,54 Å.

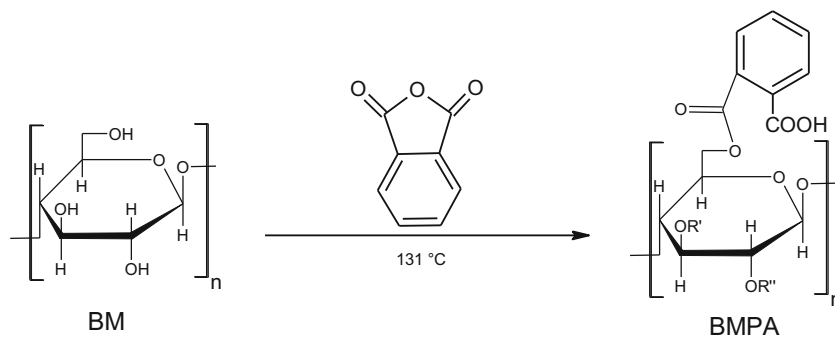
Fourier Transform Infrared Spectroscopy - FTIR

In order to characterize the presence of specific chemical groups in BMPA, and compare them with those found in BM, FTIR analyses were carried out using a KBr pellet. The spectrums were obtained using the Paragon 1000 (Perkin-Elmer, USA) in the wavelength range from 4000 to 400 cm⁻¹, with 64 sweeps at a resolution of 2 cm⁻¹.

Thermogravimetric analysis – TGA and DTG

The TGA/DTG was carried out using a Q600 V20.9 Build TA instrument, under a nitrogen atmosphere at a flow rate of

Fig. 2 Formation of BMPA by modifying *babassu mesocarp* with phthalic anhydride



100 mL min⁻¹, heating rate of 10 C° min⁻¹, and a temperature range of 25 to 800 °C.

Zeta potential analysis

The measurements of the zeta potential from the BM and BMPA were determined using a Malvern 3000 Zetasizer Nano ZS apparatus, (Malverne Instruments, UK). For the analysis of the zeta potential, the BM and BMPA solutions were first prepared in dimethylsulfoxide (DMSO). Afterwards, sulfuric acid (H₂SO₄) was added to the solution at a concentration of 0.05 mol L⁻¹, and diluted to the ratio of 1:100 (w/w).

Substrate cleaning

The substrates employed in the deposition of the films were subjected to two cleaning steps. First, they were cleaned with water and detergent, subsequently, they were cleaned using plasma. For the measurements of the cyclic voltammetry, glass substrates covered with ITO, tin oxide doped with indium, and a conductive and transparent oxide, were used.

In the first cleaning step, the substrates were initially immersed in a solution with neutral detergent and ultrapure water up to 70 °C. Thereafter, the substrates were removed and washed with Milli-Q water to remove any excess detergent. Afterwards, the substrates were immersed in ultrapure water and placed in an ultrasonic bath for 10 min. The substrates were then immersed in pure acetone, and heated for 5 min to facilitate the removal of organic matter present on their surface. Lastly, the substrates were dried and organized in a Petri dish for the next cleaning step.

Subsequently, the substrates were submitted to a plasma treatment, which was needed for the removal of any remaining impurities after the initial cleaning step. Furthermore, plasma cleaning makes the surface of the substrates more hydrophilic, and thus improves interactions between the substrate and the material of interest

[23, 24]. The parameters utilized to clean the substrates via plasma are described in Table 1.

Solution for the deposition of Self-Assembled Monolayers – SAM films

BM (1.0 mg/mL) and BMPA (1.0 mg/mL) solutions employed in the deposition of the SAM films were freshly prepared using dimethylsulfoxide (DMSO), and sulfuric acid (H₂SO₄), at a concentration of 0.05 mol L⁻¹, in a 1:6 (w/w%) proportion, respectively. These solutions were then placed in an ultrasonic bath at 25 °C for 10 min, and afterwards the pH of the solutions was adjusted to 2.85. Finally, the solutions were stored at room temperature until they were used.

Adsorption of Films by SAM technique

The adsorption procedure consisted in immersing the previously cleaned substrate in either the BM or BMPA solution for 5 min (Fig. 3). The substrate was then removed and immersed in a wash solution of ultrapure water to remove any excess natural polymer that was not adsorbed. After the washing step, the film was dried under a light N₂ flow, thereby obtaining a monolayer film of BM or BMPA; this process was repeated five times to prepare a film with five monolayers.

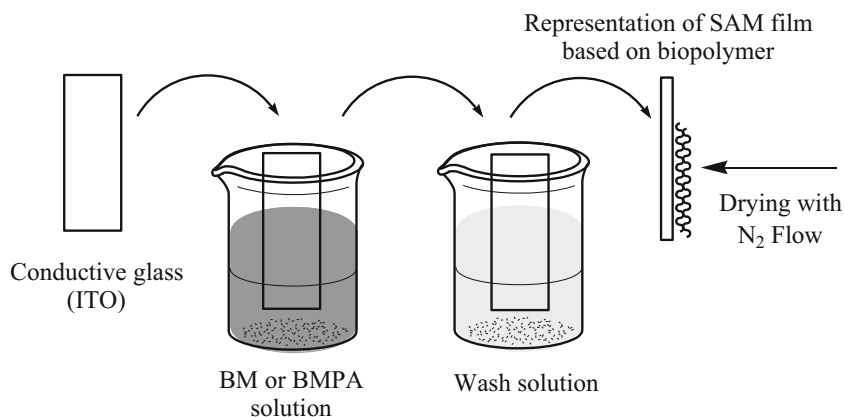
Cyclic voltammetry

The SAM films deposited on the ITO were electrochemically characterized by Cyclic voltammetry using a Dropsens μStat 400 BiPotential/Galvanostat of Metrohm apparatus, and an electrochemical cell that could fit three electrodes. A saturated calomel electrode (SCE) was employed as the reference

Table 1 Parameters used in the cleaning of the substrates via plasma

Parameters			
Plasma time	2 min	Frequency	50 kHz
Gas	Nitrogen	Pressure	200 mTorr
Gas Level	~12.5 cm ³ /min	Gas stabilization	1 min

Fig. 3 Schematic illustration of the fabrication of a SAM film containing a monolayer of BM or BMPA



electrode, a platinum spiral ($A = 2.0 \text{ cm}^2$) was used as auxiliary electrode, and the working electrode was the ITO substrate with a BM or BMPA monolayer film. The supporting electrolyte used was a H_2SO_4 aqueous solution at a 0.05 mol L^{-1} concentration.

Scanning electron microscope – SEM

The morphology of the obtained films was evaluated using a scanning electron microscope (JSM 6360LV, JEOL/Noran). The images were collected using acceleration voltages of 15 and 30 kV. Before their examination, the samples were covered with a thin gold layer by sprinkling using a low deposition rate, cooled, and placed at a maximum distance away from target in order to avoid their damage.

Atomic Force Microscopy

Representative films were examined using AFM. The analysis was carried on the samples in vibrating (tapping) mode. Imaging was performed using a TT-AFM instrument (AFM Workshop). All images were collected at 512 pixel resolution for a $4 \times 4 \mu\text{m}$ area, and at least three different areas were examined per sample. Representative data are shown. The images have been processed, analyzed, and displayed using Gwyddion 2.29 software. The roughness values shown are for the $4 \times 4 \mu\text{m}$ areas and represent the roughness average (Ra) values.

Results and discussions

Characterization

The acid groups of BM and BMPA was determined by retro-titration, where BM and BMPA presented values of $43.3 \pm 0.82 \text{ mg g}^{-1}$, and $154.67 \pm 0.77 \text{ mg g}^{-1}$, respectively, after the phthalation reaction. This increase in the BM substitution capacity after phthalation occurred due to an increase in the

number of active sites with the incorporation of the groups present in phthalic anhydride [25, 26].

The XRD peaks of the PA, BM and BMPA samples are shown in Fig. 4a. The XRD pattern for BM suggests the presence of a lignocellulosic polymer, which also presents starch

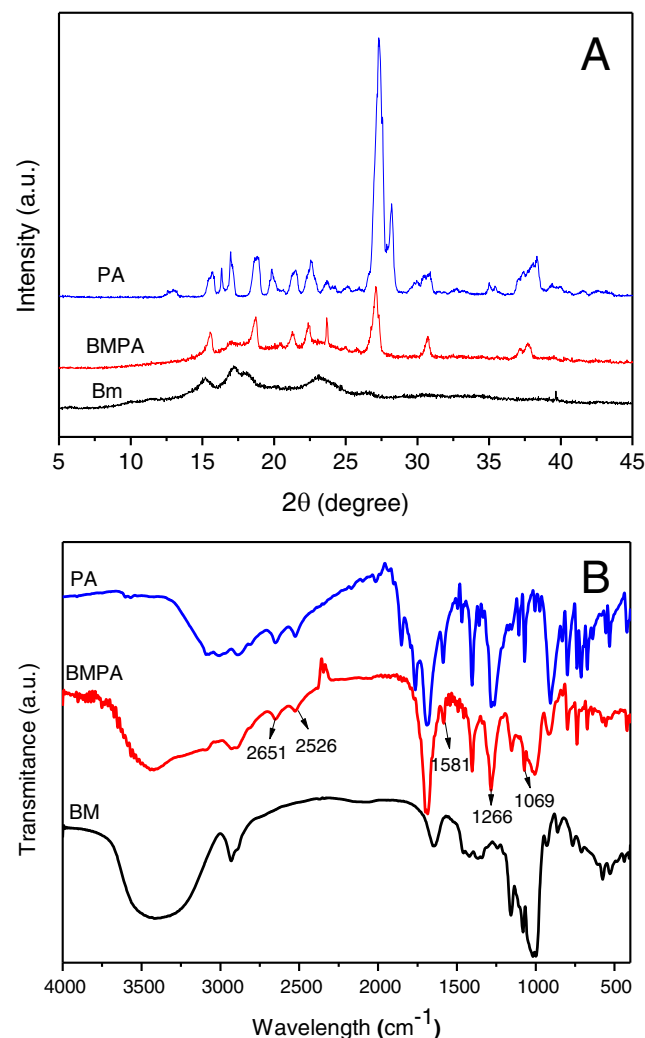


Fig. 4 a) XRD patterns of PA, BM, and BMPA and b) shows FTIR spectra of PA, BM, and BMPA

in its composition, with defined diffraction peaks at $2\theta = 15.6^\circ$, 17.2° , and 23.1° [27].

The diffraction peak in BM at $2\theta = 23.1^\circ$ is characteristic of crystalline-type cellulose [28]. On the other hand, the two peaks at $2\theta = 15.6^\circ$ and 17.2° in BM appeared when the cellulose content was high, and contained a high amount of amorphous components such as lignin, hemicellulose, and amorphous cellulose [29].

BMPA diffractogram showed new peaks, highlighting the peak $2\theta = 38.3^\circ$, besides the displacement of the characteristic peaks of the AP at $2\theta = 18.7^\circ$ to 18.6° ; 21.4° to 21.2° ; 22.5° to 22.3° ; 27.1° to 27.0° and 37.6° to 37.4° . The observed change reported that the incorporation of phthalic anhydride occurred in the crystalline part of the biopolymer, as observed in similar studies [30, 31].

The increase in the BMPA crystallinity in relation to BM was expected, since during the modification of BM with PA, the removal of most of the compounds (lignin and hemicelluloses) responsible for the amorphous portion of BM can occur [32, 33]. The X-ray diffractogram of BMPA showed that after each step of the surface modification process, there was a change in its crystalline profile. In addition to the diffraction peaks characteristic of the structure of the BM sample, we can also observe the characteristic diffraction peaks of PA, which confirms the efficiency of the modification reaction. It can also be seen that after the modification with PA, the XRD pattern for BMPA does not exhibit the baseline peak of PA.

The modifications are expected to first occur on the hydroxyl groups of the crystalline region, located on the polymer surface. After the rearrangement of the surface, new crystallographic patterns appeared due to aromatic-aromatic interactions in PA [20].

In Fig. 4b, the observed band in BM at 3420 cm^{-1} is related to O-H stretching from the hydroxyl groups of polysaccharides and carboxyl groups of acids. Furthermore, vibrations related to the C-H group in BM appeared at around 2922 cm^{-1} , and the axial deformation that corresponds to this group was observed at 1415 and 1372 cm^{-1} [34, 35].

The bands at 1330 cm^{-1} in the BM come from guaiacyl-syringyl ring vibrations [36]. The bands at 1012 cm^{-1} of BM come from the C-O-C group vibration of the pyranose ring of the polysaccharide monomer. The observed bands below 1000 cm^{-1} are generally associated to the absorption of the hydroxylic groups in the polysaccharide monomer [32].

After modifying BM with PA, characteristic bands of the modification process were observed. The band at 2897 cm^{-1} in the BMPA arises from the bond between the carbon of the biopolymer and the intramolecular hydrogen of the acidic group of PA. The bands at 2651 and 2526 cm^{-1} in BMPA are related to dimers of the aromatic carboxylic acids present in PA [20].

The most intense MBAF band around 1691 cm^{-1} is related to the C=O group present in the PA structure.

The bands at 1581 , 1470 , and 1411 cm^{-1} , which appeared in the BMPA spectrum, are related to vibrations of the

aromatic ring from the lignin, specifically the guaiacyl ring, related to (C-H) plan from ortho-disubstituted benzene in PA, that, although the mesocarp is mostly constituted of starch, it still has other polymers as lignin e hemicellulose. The band at 1266 cm^{-1} corresponds to the associated C-O bond of the aromatic ester group, which is formed from the bond between the carbon 6 of the starch present in the biopolymer, preferably with the acidic group of PA [20–39].

The modification of the surface of the BMPA also causes the appearance of a band at 1069 cm^{-1} related to the stretch of the C-O group in the cellulose or starch monomer, which is found in hemicellulose and lignin. This band at 1069 cm^{-1} suggests the effective participation of the glycosidic bonds $\beta(1 \rightarrow 4)$ present in BMPA, involving π - π aromatic-aromatic interactions of PA [38, 39].

The spectrum for BMPA showed common bands to both BMPA and PA, indicating the successful phthalation of BM. The presence of these bands possibly indicates that the anhydride molecules were successfully incorporated into the structure of BMPA.

The TGA curves provided information about the thermal stability of the samples, as illustrated in Fig. 5.

In the TGA/DTG curves presented in Fig. 5a and b three stages of decomposition for BM are observed, and this same behavior has been observed by Mulinari et al. [40]. The first

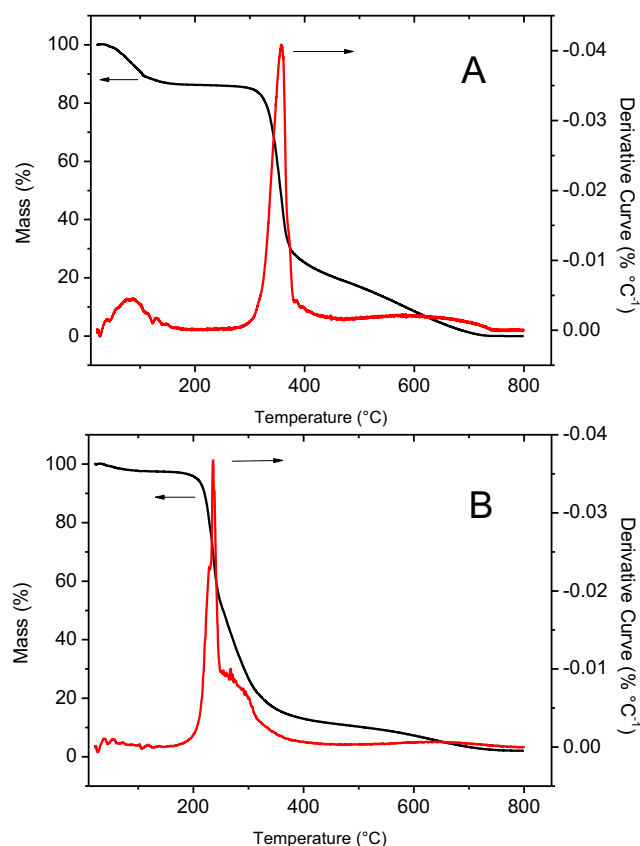


Fig. 5 TG/DTG curves of (a) BM and (b) BMPA

mass loss, about 14%, occurred in the temperature range between 25 and 140 °C, and is attributed to the removal of volatiles and physisorbed water [41]. The second stage of mass loss, at 57%, in the temperature range of 140 to 370 °C, was associated with the beginning of the thermal degradation of the hemicellulose (starch and lignin) [42, 43]. The third, last stage of mass loss occurs from 370 °C to 800 °C, with a mass loss of 29%, attributed to the final degradation of the BM structure.

The decomposition of the BMPA happened in four stages. The first stage of decomposition was attributed to the liberation of physically adsorbed water on the surface of the material and synthesis residue, occurring from 25 °C to 180 °C, with a 4% mass loss, being observed a greater mass variation than the starting material, since this material has a lower affinity for water, becoming less hydrophilic after modification. The second decomposition occurred from 180 °C to 235 °C with a 30% mass loss, where the degradation of the modified group occurred, creating a variety of oxidative processes and interactions. The third stage is related to the thermal degradation of the lignin bonds, and the partial degradation of BMPA, which happened in the range from 235 to 409 °C, with a 55% mass loss. The fourth and last stage occurred in the range from 409 °C to 800 °C, with an 11% mass loss, and is associated with the final degradation of the BMPA structure. The DTG curves for the BM and BMPA polymers (Fig. 5a, b) show that maximum degradation occurred at around 350 °C and 235 °C, respectively. This alterations refers to the rupture of inter and intramolecular hydrogen bonds between the hydroxyl groups of the precursor material, which occurs after the reaction with the anhydride, becoming weaker bonds and less intense between the groups present on the surface in the final material.

Figure 6 shows the micrographs of BM and BMPA. The BM micrograph, Fig. 6a, reveals the presence of polygonal oval format granules (characteristics of the starch), without structural damage and of different sizes. It is also observed that these granules form agglomerates, possibly due to the presence of lignin and starch in the BM structure. The

BMPA micrograph, Fig. 6b, crystalline formations are observed on the surface of the granules, suggesting that the surface of the BM was modified by phthalic anhydride.

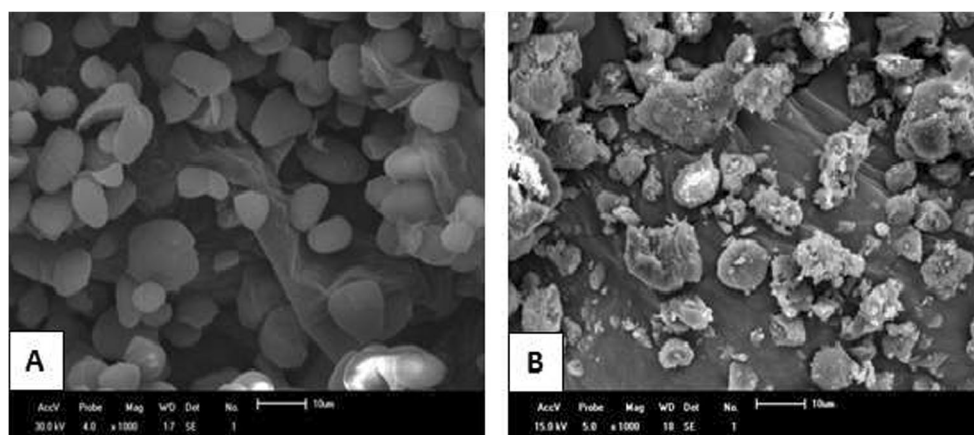
The BM and BMPA solutions prepared with dimethylsulfoxide (DMSO) and sulfuric acid (H_2SO_4 , 0.05 mol L^{-1}) were characterized by their zeta potential, under the same conditions used for the thin film formation, in order to check the loads of these solutions. The results from the zeta potential showed a medium superficial charge value of -16.3 mV for BM, and -4.73 mV for BMPA. These superficial charge values were negative due to the esterification of the hydroxyls in BMPA, which are anionic [44], and with the replacement of the OH- groups by PA, the value of the zeta potential becomes smaller for BMPA, as expected.

Characterization of monolayer films of BM and BMPA by cyclic voltammetry

Figure 7a shows the cyclic voltammogram of five different monolayer films of ITO/BM and ITO/BMPA. For comparison, the voltammogram of a non-modified substrate was also considered under the same experimental conditions, and in this case, no electroactive behavior was observed.

The cyclic voltammogram obtained for monolayer films of BM and BMPA, deposited on an ITO electrode, Fig. 7a, showed an electroactive behavior in a supporting electrolyte solution of $0.05 \text{ mol L}^{-1} \text{ H}_2\text{SO}_4$. The BM film presented an oxidation process at $+0.57 \text{ V vs SCE}$, while a reduction process was observed at $+0.19 \text{ V vs SCE}$. Although both BM and BMPA presented electroactivity, however, the modification realized on biopolymer resulted in a higher definition and reversibility of redox process of BMPA, as shown in Fig. 7a. In other words, after the modification of the polymer, the oxidation potential of the BM film, previously observed at $+0.57 \text{ V vs SCE}$, was displaced to $+0.37 \text{ V vs SCE}$, while the reduction potential moved from 0.19 V vs SCE to 0.24 V vs SCE , as seen in Fig. 7a. In short, it was observed that the modification of the biopolymer with phthalic anhydride improved its electroactivity, and facilitated

Fig. 6 Scanning electron micrographs of (a) BM and (b) BMPA



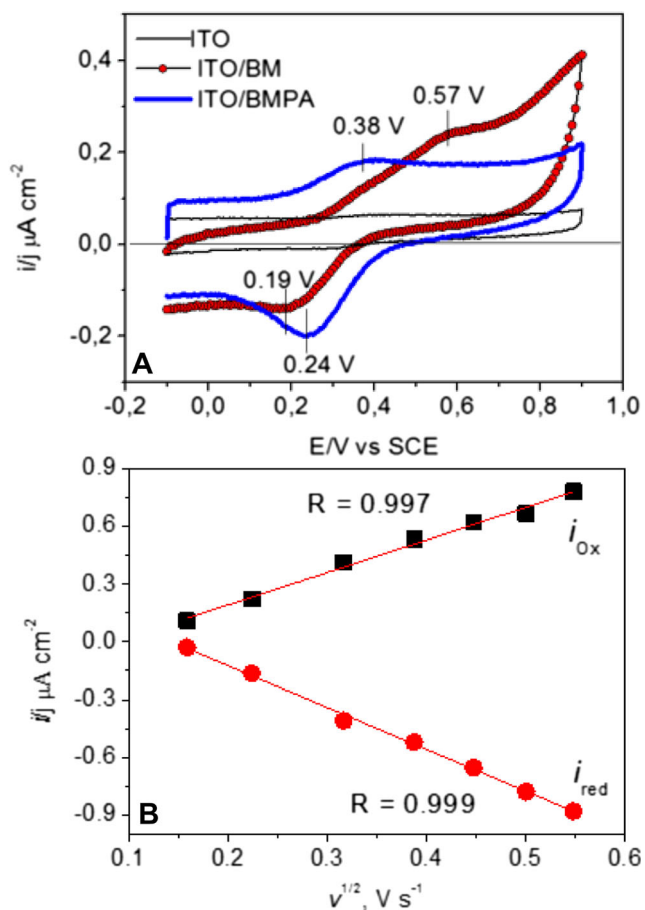


Fig. 7 (a) Cyclic voltammograms comparing the influence of modification with Phthalic anhydride on the electrochemical response of *babassu mesocarp*. (b) Anodic and cathodic peak current dependence by the square root of scan rate obtained for the BMPA films. All voltammograms were obtained in a $0.05 \text{ mol L}^{-1} \text{ H}_2\text{SO}_4$ solution for $v = 50 \text{ mV s}^{-1}$

its oxidation process in a 0.05 mol L^{-1} aqueous H_2SO_4 solution. This increments the advantages of the modification of this material for its use as an active layer of electrochemical sensors.

Following this perspective, and seeking to assess the feasibility of the suggested application, the electrochemical mechanism of BMPA was investigated (Fig. 7b). The Fig. 7b shows the current dependence of the anodic (i_{ox}) and cathodic (i_{red}) peaks of the BMPA film, as a function of the square root of the scan rate BMPA. This behavior indicates that the monolayer film of BMPA had an electrochemical mechanism controlled by diffusion processes [45].

Table 2 presents the data from the electrochemical reversibility of the BM and BMPA monolayer films deposited on ITO electrode. In a reversible reaction, the peak current should vary linearly with the square root of the scan rate, or the ratio of cathodic and anodic peak current must be equal to one [46, 47]. The lower the value between the E_{Ox} and E_{Red} potentials, the more reversible the reaction, and when the ratio between the current of the anodic (I_{Ox}) and cathodic (I_{Red}) processes is

Table 2 Reversibility System BM and BMPA

Biopolymer	$E_{\text{Ox}} - E_{\text{Red}}$ (mV)	$I_{\text{Ox}} / I_{\text{Red}}$
BM	330	1.78
BMPA	140	0.93

closer to 1, the response is more electrochemically reversible [45]. Thus, the results shown in Table 2 confirm that the BM modification improved the electrochemical reversibility of the biopolymer.

Figure 8a and b present the results of the electrochemical stability of the BM and BMPA monolayer films, respectively. Generically, it was observed that the ITO/BMPA film had a better stability than the ITO/BM film. This event can be associated with an improved reversibility of the redox process in the polymer after its modification.

In Fig. 8a it can be observed that after the first cycles there was a sharp decline in the chain density of the BM oxidation process, set at $+0.57 \text{ V}$ vs SCE, followed by the total disappearance of this process after the third consecutive scan

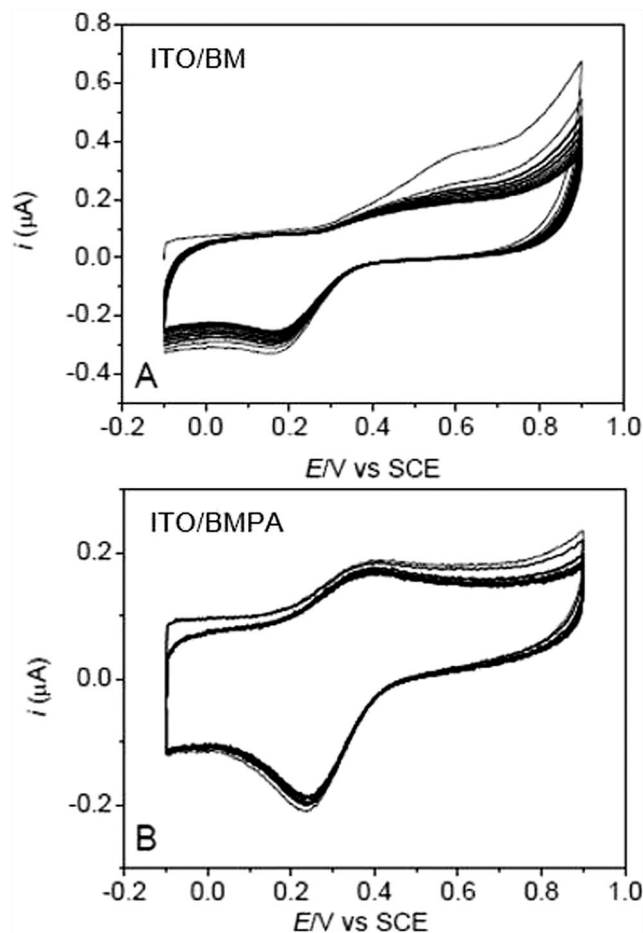
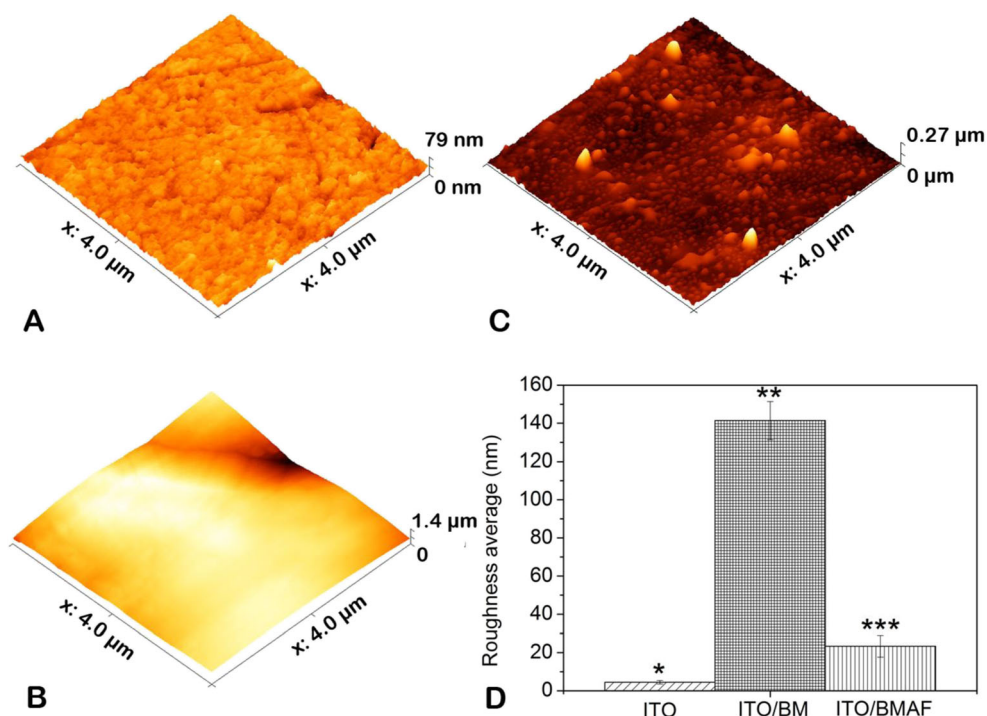


Fig. 8 Consecutive cyclic voltammograms (20 cycles) comparing the electrochemical stability of (a) BM and (b) BMPA. All voltammograms were obtained in an H_2SO_4 solution at a concentration of 0.05 mol L^{-1} , and with $v = 50 \text{ mV s}^{-1}$

Fig. 9 Dynamic-mode AFM images of glass surfaces covered with a) ITO, SAM films of b) ITO/BM and c) ITO/BMPA. d) Shows a comparison between the roughness average values of different surfaces studied. All images are $4.0 \times 4.0 \mu\text{m}$ in x and y



consecutive. Furthermore, there was no stabilization of the current. This suggests that it is not practicable the use non-modified BM in electrochemical sensors. On other hand, in Fig. 8b, it can be observed in the BMPA voltammogram that after the third cycle there tended to be a faster stabilization of the current, in addition to a conservation of the oxidation and reduction processes for 20 successive cycles. These results show that although the BMPA redox process is not totally reversible, it is quite stable in the employed experimental conditions, and thus it justifies the use of this system as an electrochemical sensor in future applications.

Morphological characterization of SAM films by AFM

Figure 9 shows representative images of the surface of an unmodified ITO electrode (Fig. 9a) or modified with a SAM film of BM (Fig. 9b) or BMPA (Fig. 9c). Figure 9d shows a comparative graph between the surface roughness of the different surfaces studied.

The morphology observed for ITO is well-known and highly characteristic microstructure, which has been observed by AFM many times before, for example in EATON and WEST [48]. This structure, shown in Fig. 9a, consists of somewhat flat “islands”; each covering areas of 100 nm^2 up to $1.0 \mu\text{m}^2$ made up of many small ($< 40 \text{ nm}$) globular grains, which stand above similar globular grains at a lower level [49].

The BM film exhibited a morphology with total ITO coating by large BM grains, which made it difficult the characterization by AFM, which is a technique for observing very small areas. SAM films are prepared from the solutions of the

materials of interest and, since BM has low solubility in aqueous media, the formation of these large grains is favored. On the other hand, the SAM film of BMPA presented a very distinct morphology, with grains of size varying between 40 and 260 nm, distributed throughout the surface of the ITO. Certainly, the smaller size of these grains facilitates the transport of charges at the electrode/electrolyte interface, which corroborates with the data obtained by cyclic voltammetry.

An analysis of the average roughness of the surface of these films was performed and obtained values of $4.48 \pm 0.98 \text{ nm}$, $141.4 \pm 10.21 \text{ nm}$ and 23.3 ± 5.67 , for ITO, ITO/MB and ITO/BMPA, respectively, Fig. 9d.

Conclusion

The modification in babassu mesocarp with phthalic anhydride was confirmed by different techniques.

In the cyclic voltammetry analysis, both BM and BMPA presented electroactivity in acidic environments; however, the response of the modified polymer presented a better-defined redox process, and a higher reversibility and electrochemical stability. In the stability analysis, it was confirmed that the BM modification increased the system’s stability in the employed experimental conditions. This justifies the possibility of using of the BMPA system as an electrochemical sensor.

According to the results from the voltammetry analysis, this study proved the electroactivity of BM and BMPA polymers, and BMPA in the form of monolayer films exhibited suitable electrochemical properties for use in the construction

of electrochemical sensors. However, the BMPA film presented better electrochemical response, since the modification of BM improves its solubility, favoring the preparation of films with smaller grain sizes, as observed by AFM.

Acknowledgements The authors thank to Coordination Support in Higher Education (CAPES), National Council for Scientific and Technological Development (CNPq), and the Foundation of Support to Research of Piauí (FAPEPI) for their financial support; and The Federal University of Piauí (UFPI), and Federal Institute of Piauí (IFPI) for providing the work research conditions.

Compliance with ethical standards

Conflict of Interest The authors declare that they have no conflict of interest.

References

- Rao MG, Bharathi P, Akila RM (2014) A Comprehensive Review On Biopolymers. *Sci Rev Chem Commun* 4(2):61–68
- Zhang J, Mungara P, Jane J (2001) Mechanical and thermal properties of extruded soy protein sheets. *Polym* 42(6):2569–2578
- Yates MR, Barlow CY (2013) Life cycle assessments of biodegradable, commercial biopolymers-A critical review. *Resour. Conserv Recycl* 78:54–66
- Finkenstadt VL (2005) Natural polysaccharides as electroactive polymers. *Appl Microbiol Biotechnol* 67(6):735–745
- Prabaharan M (2008) Review paper: Chitosan derivatives as promising materials for controlled drug delivery. *J Biomater Appl* 23(1): 5–36
- Jayakumar R, Prabaharan M, Reis RL, Mano JF (2005) Graft copolymerized chitosan present status and applications. *Carbohydr Polym* 62(2):142–158
- Carpenter AL, Lannoy CF, Wiesner MR (2015) Cellulose nanomaterials in water treatment technologies. *Environ Sci Technol* 49(9):5277–5287
- Raquez JM, Habibi Y, Murariu M, Dubois P (2013) Polylactide (PLA)-based nanocomposites. *Prog Polym Sci* 38(10–11):1504–1542
- Lee J (1997) Biological conversion of lignocellulosic biomass to ethanol. *J Biotechnol* 56(1):1–24
- Lorenzi, H. (2010). *Flora brasileira Lorenzi: Arecaceae (palmeiras)*. 1 ed. São Paulo: Nova Odessa, 367p
- Albiero D, Maciel AJS, Lopes AC, Mello CA, Gamero CA (2007) Proposal of harvest's babaçu machine (*Orbignya phalerata* Mart.) for the small farms. *Acta Amazon* 37(3):337–346
- Vieira AP, Santana SAA, Bezerra CWB, Silva HAS, Chaves JAP, Melo JCP, Silva Filho EC, Airoidi C (2009) Kinetics and thermodynamics of textile dye adsorption from aqueous solutions using babassu coconut mesocarp. *J Hazard Mater* 166(2–3):1272–1278
- Liu CF, Sun RC, Zhang AP, Ren JL, Wang XA, Qin MH, Chao ZN, Luo W (2007) Homogeneous modification of sugarcane bagasse cellulose with succinic anhydride using a ionic liquid as reaction medium. *Carbohydr Res* 342(7):919–926
- Santana SAA, Vieira AP, Silva Filho EC, Melo JCP, Airoidi C (2010) Immobilization of ethylenesulfide on babassu coconut epicarp and mesocarp for divalent cation sorption. *J Hazard Mater* 174(1–3):714–719
- Teixeira PRS, Marreiro ASN, Farias EAO, Dionisio NA, Silva Filho EC, Eiras C (2015) Layer-by-layer hybrid films of phosphate cellulose and electroactive polymer as chromium (VI) sensors. *J. Sol. State Electrochem* 19(7):2129–2139
- Alves OL, Ronconi CM, Galembeck A (2002) Decomposição de precursores metalorgânicos: uma técnica química de obtenção de filmes finos. *Quim Nova* 25(1):69–77
- Ulman A (1991) Thermal-stability of lagmuir-blodgett and self-assembled films a possible scenario for order-disorder transitions. *Adv Mater* 3(6):298–303
- Samanta D, Amitabha Sarkar A (2011) Immobilization of biomacromolecules on self-assembled monolayers: Methods and sensor applications. *Chem Soc Rev* 40:2567–2592
- Freire RS, Pessoa CA, Kubota LT (2003) Emprego de monocamadas auto-organizadas no desenvolvimento de sensores eletroquímicos. *Quim. Nova* 26(3):381–389
- Melo JCP, Silva Filho EC, Santana SAA, Airoidi C (2009) Maleic anhydride incorporated onto cellulose and thermodynamics of cation-exchange process at the solid/liquid interface. *Colloids Surf A Physicochem Eng Asp* 346(1–3):138–145
- Vieira AP, Santana SAA, Bezerra CWB, Silva HAS, Melo JCP, Silva Filho EC, Airoidi C (2010) Copper sorption from aqueous solutions and sugar cane spirits by chemically modified babassu coconut (*Orbignya phalerata Marteciosa*) mesocarp. *Chem Eng J* 161(1–2):99–105
- Zhou Y, Min Y, Qiao H, Huang Q, Wang E, Ma T (2015) Improved removal of malachite green from aqueous solution using chemically modified cellulose by anhydride. *Int J Biol Macromol* 74:271–277
- Finson, E., Kaplan, S. L. & Wood, L. (1995). *Plasma Treatment of Webs and Films*, Society of Vacuum Coaters, 38th Annual Technical Conference Proceedings
- Petasch W, Kegel B, Schmid H, Lendenmann K, Keller HU (1997) Low-pressure plasma cleaning: a process for precision cleaning applications. *Surf Coat Technol* 97(1–3):176–181
- Bezerra RDS, Silva MMF, Morais AIS, Osajima JA, Santos MRMC, Airoidi C, da Silva Filho EC (2014) Phosphated cellulose as an efficient biomaterial for aqueous drug ranitidine removal. *Mater* 7(12):7907–7924
- Rungrodnimitchai S (2014, 2014) Rapid preparation of biosorbents high ion exchange capacity from rice straw and bagasse for removal heavy metals. *Sci. World. J.:*1–9
- Salmon S, Hudson SM (1997) Crystal morphology, biosynthesis, and physical assembly of cellulose, chitin, and chitosan. *J. Macromol. Sci., Part C: Polym. Rev* 37(2):199–276
- Tserki, V., Matzinos, P.; Kokkou, S., Panayiotou, C. (2005) Novel biodegradable composites based on treated lignocellulosic waste flour as filler. Part I Surface chemical modification and characterization of waste flour Compos Part A 36, 965–974
- Vieira AP, Santana SAA, Bezerra CWB, Silva HAS, Chaves JAP, Melo JCP, da Silva Filho EC, Airoidi J (2011) Epicarp and mesocarp of Babassu (*Orbignya speciosa*): Characterization and application in copper phtalocyanine dye removal. *J Braz Chem Soc* 22(1):21–29
- Zhou Y, Min Y, Qiao H, Huang Q, Wang E, Ma T (2015) Improved removal of malachite green from aqueous solution using chemically modified cellulose by anhydride. *Int. J Biol Macromol* 74(1):271–277
- Zhou Y, Jin Q, Hu X, Zhang Q, Ma T (2012) Heavy metal ions and organic dyes removal from water by cellulose modified with maleic anhydride. *J Mater Sci* 47:5019–5029
- Ass BAP, Ciacco GT, Frollini E (2006) Cellulose acetates from linters and sisal: correlation between synthesis conditions in DMAc/LiCl and product properties. *Bioresour Technol* 97(14): 1696–1702
- Fung KL, Xing XS, Li RKY, Mai YW (2003) An investigation on processing of sisal fibre reinforced polypropylene composites. *Compos. Sci. Technol* 63(9):1255–1258

34. Qiu K, Yang J (2010) Preparation and actividad carbons walnut shells via vacuum chemical activation and their application for methylene blue removal. *Chem Eng J* 165(1):209–217
35. Tang Y, Qiang L, Chen F (2012) Preparation and characterization of actividad carbon from waste ramulus mori. *Chem Eng J* 230(1):19–24
36. Abreu HS, Oertel AC (1999) Estudo químico da lignina de *Paullinia rubiginosa*. *Cerne* 5(1):52–60
37. Jorgensen WL, Severance DL (1990) Aromatic–aromatic interactions: free energy profiles for the benzene dimer in water, chloroform and liquid benzene. *J Am Chem Soc* 112(12):4768–4774
38. Yang CQ, Wang X (1996) Formation of cyclic anhydride intermediates and esterification of cotton cellulose by multifunctional carboxylic acids: An infrared spectroscopy study. *Text Res J* 66(9):595–603
39. Liu CF, Sun RC, Ye J (2006) Structural and thermal characterization of sugarcane bagasse phthalates prepared with ultrasound irradiation. *Polym Degrad Stab* 91(2):280–288
40. Mulinari, D. R., Cruz, T. G., Cioffi, H. O. M., Voorwald, H. J. C., Da Silva, M. L. C. P. & Rocha, G. J. M. (2010). Image analysis of modified cellulose fibers from sugarcane bagasse by zirconium oxychloride. *Carbohydr Res*, 345(13), 1865–1871
41. Szczesniak L, Rachocki A, Tritt-Goc J (2008) Glass transition temperature and thermal decomposition of cellulose powder. *Cellulose* 15(3):445–451
42. Antich P, Vázquez A, Mondragon I, Bernal C (2006) Mechanical behavior of high impact polystyrene reinforced with short sisal fibers. *Compos A: Appl Sci Manuf* 37(1):139–150
43. Yang H, Yan R, Chen H, Lee DH, Zheng C (2007) Characteristics of hemicellulose, cellulose and lignina pyrolysis. *Fuel* 86(12–13): 1781–1788
44. Mirhosseini H, Tan CP, Hamid NSA, Yusof S (2008) Effect of Arabic gum, xanthan gum and orange oil contents on zeta-potential, conductivity, stability, size index and pH of orange beverage emulsion. *Colloids Surf.A Physicochem Eng Asp* 315(1–3):47–56
45. Bard, A.J. & Faulkner, L.R. (2001). *Electrochemical methods fundamentals and applications*. New York: John Wiley & Sons
46. Wang, J. (2000). *Anal. Electrochem.* (2th. ed.). New Jersey: Wiley-VCH
47. Scholz F (2010) *Electroanalytical Methods Guide to Experiments and Applications*. Springer Verlag, Berlin
48. Eaton P, West P (2010) *Atomic Force Microscopy*. Oxford University Press. Oxford, UK
49. Farias EAO, Santos MC, Dionisio NA, Quelemes PV, Leite JRSA, Eaton P, Silva DA, Eiras C (2015) Layer-by-Layer films based on biopolymers extracted from red seaweeds and polyaniline for applications in electrochemical sensors of chromium VI. *Mater Sci Engin. B* 200:9–21